Japanese Journal of Applied Physics **53**, 03DB01 (2014) **REGULAR PAPER**
http://dx.doi.org/10.7567/JJAP.53.03DB01

Relationship between center-peaked plasma density profiles and harmonic electromagnetic waves in very high frequency capacitively coupled plasma reactors

Ikuo Sawada[1*], Peter L. G. Ventzek[2], Barton Lane[2], Tatsuro Ohshita[3], Rochan R. Upadhyay[4], and Laxminarayan L. Raja[5]

[1]*Tokyo Electron U.S. Holdings, Inc., Austin, TX 78741, U.S.A.*
[2]*Tokyo Electron America, Austin, TX 78741, U.S.A.*
[3]*Tokyo Electron Miyagi, Taiwa, Miyagi 981-3629, Japan*
[4]*Esgee Technologies Inc., Austin, TX 78746, U.S.A.*
[5]*The University of Texas Austin, Austin, TX 78712, U.S.A.*
E-mail: isawada335@cf6.so-net.ne.jp

Received September 3, 2013; revised December 6, 2013; accepted December 24, 2013; published online March 5, 2014

An understanding of the factors that control radial plasma uniformity in very high frequency (VHF) capacitively coupled plasma (CCP) sources is important for many plasma processes in semiconductor device manufacturing. Here, we report experimental measurements and high-resolution self-consistent numerical simulations that illustrate the plasma density profile and the higher harmonic wave content in two types of VHF-CCP test-bench reactors. A distinct sharp center peak superimposed on a broad center peak in argon plasma was observed for driving frequencies of 60 and 106 MHz. Experimental measurements and numerical simulations of the electric field power spectrum reveal the presence of UHF waves when the electron density is over 5×10^{16} (#/m^3). The presence of UHF waves closely correlates with the occurrence of a distinct and sharp-center-peaked electron density. The numerical simulations show that specific frequency bands in the UHF spectrum are amplified in the plasma and lead to the evolution of the sharp-center-peaked electron density. © 2014 The Japan Society of Applied Physics

1. Introduction

Very high frequency (VHF) capacitively coupled plasma (CCP) sources are now widely used as plasma etching and plasma-enhanced chemical vapor deposition (PECVD) tools for manufacturing semiconductor wafers and flat panel displays. The primary benefits of using VHF-CCP sources are efficient plasma generation at very high frequencies (30–300 MHz), stable operation with low plasma potential, and the ability to decouple ion acceleration to the wafer from plasma generation processes. However, the plasma tends to become radially nonuniform or possess a center-peaked plasma density profile when VHF plasma sources are employed. This nonuniformity is generally associated with the reduced wavelength of electromagnetic waves that are established in these sources and the ratio of this wavelength to the chamber electrode dimensions as originally described by Stevens and coworkers.[1)] Therefore, understanding how the plasma uniformity evolves is important as the wafer diameter increases from 300 to 450 mm.

Numerous experimental reports on the radial distribution of plasma density or the associated physical properties in simple-structure parallel-plate CCP sources have shown that center-peaked plasma properties (density, current, and optical emission) occur when the driving frequency exceeds tens of MHz. Induction probe measurements of the RF current profile reported by Hebner and coworkers[2,3)] showed that the RF current at the center is higher for a high driving frequency of 176 MHz than for 13.56 MHz. Sung and coworkers[4,5)] measured the profile of Ar line (750 nm) emission intensity in a 100 MHz CCP source. Assuming a relatively uniform electron temperature profile, reasonable at low pressures, they concluded that the measured center-peaked optical emission data indicated a center-peaked electron density profile. Plasma absorption probe (PAP) measurements[6–9)] of electron densities in argon plasmas also showed that the center-peaked plasma density profile was more pronounced at a driving frequency of 60 MHz although the density profile depended on matching circuit settings.

Several hypotheses have been established to explain the cause of the center-peaked plasma profile in VHF-CCP systems. One hypothesis, perhaps the first, is that the standing wave phenomenon[10)] from the driving fundamental excitation frequency causes a nonuniform center-peaked electric field in the plasma sheaths over the electrodes, which in turn provides increased heating (stochastic and Ohmic) around the center. Lee and coworkers[11)] determined the plasma density using a coupled simulation with ambipolar plasma transport, analytic plasma sheaths, and frequency-domain electromagnetic wave models. They considered only the fundamental frequency as part of the frequency-domain electromagnetic wave description in their work, but they showed that the plasma could be center-peaked at frequencies above 80 MHz. Another hypothesis is that waves with frequencies higher than the fundamental frequency in plasma induce the prominent heating around the center. Miller and coworkers[3)] measured the generation profile of the higher harmonic waves in plasma using a B-dot probe. Around the center, the presence of ultrahigh frequency (UHF) waves of over 300 MHz in the case of 60 MHz feed and those of over 500 MHz in the case of 176 MHz feed was notable. Importantly, a center-peaked optical emission profile was observed when UHF waves were present in the plasma. Also, with respect to the role of harmonics of the fundamental, a variety of explanations exist. For example, nonlinearity in the sheath impedance is attributed to the growth of higher harmonic waves by fundamental excitation,[12,13)] while others attribute the plasma series resonance (PSR) phenomenon where the plasma coupled with the external circuit produces harmonics of the fundamental to be generated.[14–19)]

Many numerical simulations of plasma density profiles in facsimiles of commercial-scale VHF-CCP tools have been reported.[20–25)] In addition to the aforementioned simulations by Lee and coworkers, other numerical simulations include

coupled solutions of the plasma fluid and the time domain electromagnetic fields. The models used have the necessary physics components for predicting the generation of higher harmonics, but no report of their existence was made. The coarse spatial resolution of the computational mesh in these studies leads to a significant numerical diffusion. Numerical diffusion would effectively eliminate higher harmonic waves from the solution.

The test-bench reactors are geometrically simpler than typical commercial tools they try to mimic but include all the relevant hardware components pertinent to reproducing the center-peaked electron density in VHF-CCP sources. In our previous work,[26] we found that there is a strong correlation between the calculated harmonic waves and the sharp center peak of electron density in test-bench A. In this report, results from concurrent experimental and simulation studies of two test-bench VHF-CCP reactor systems are presented. Both the measured electron density profiles and the frequency spectrum of the electric field within the plasma for two systems are reported. The computational simulations are performed with a very high spatiotemporal resolution of the plasma and wave phenomena accompanied by the addition of higher harmonics perturbation, and enable us to describe the relationship between the center-peaked phenomena observed in VHF-CCPs and the higher harmonic waves amplified in the plasma. The obtained results clearly indicate that the plasma uniformity and higher harmonic wave phenomena are unambiguously linked.

2. Experiment and computational simulation

2.1 Experiment

Electron density profiles were measured using a PAP that is described in detail elsewhere.[8,9] Briefly, the PAP measurement relies on the fact that microwave electric fields have an absorption threshold at the plasma frequency. The identification of the absorption threshold allows the identification of the plasma density. In practice, a coaxial cable is passed through a quartz tube suspended in the chamber. The tip of the exposed cable, the shape of which is a rod, interacts with the plasma through the quartz tube. The measurement of the absorption of a weak injected electromagnetic wave as a function of frequency allows the identification of the plasma frequency and therefore the electron density.

Two test-bench reactors were used in this study: test-bench A (60 MHz) and test-bench B (106 MHz), both with simple parallel plate structures. Figures 1 and 2 show schematics of the CCP test-bench A and B, respectively. Apart from the driving frequencies, the primary distinction between the two sources is the existence of a large open space at the periphery of the chamber in test-bench A. Test-bench B has a ground plane nearer the wafer subsector edge. The ground plane is porous, allowing gas to pass into and out of the stagnant (flow-free) plasma region. The flow conditions in the test benches are different, but we do not expect flow to play an important role in the results. The key specifications are listed in Table I. In both experiments, the configuration and power were set such that the electron densities measured were typical of those measured for similar plasmas in commercial VHF-CCP sources.

The higher harmonic electromagnetic wave content in the plasma bulk was also measured in test-bench B (106 MHz)

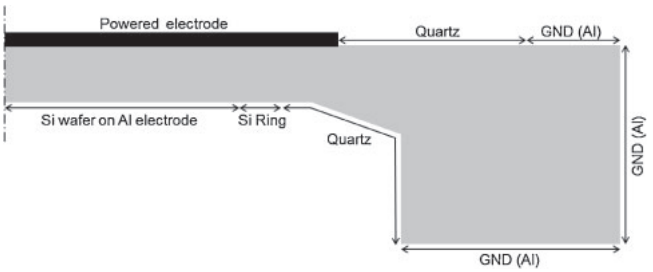

Fig. 1. Schematic illustration of capacitively coupled plasma test-bench A.

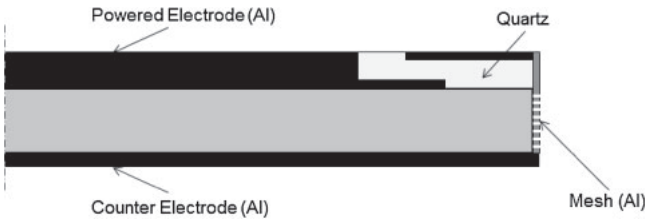

Fig. 2. Schematic illustration of capacitively coupled plasma test-bench B.

Table I. Key specifications in CCP test-bench A and test-bench B.

	Test-bench A	Test-bench B
Gap between electrodes (mm)	25	25
Chamber diameter (mm)	520	380
Powered electrode diameter (mm)	320	280
Drive frequency (MHz)	60	106
Gas and pressure (mTorr)	Ar 15, 100	Ar 40, 100

using a PAP for VHF powers of 100–400 W and pressures of 20–100 mTorr. In these measurements,[9] the probe was set in the plasma as a passive antenna to measure the full range of electromagnetic waves in the plasma bulk. The measured signals are relative and there was no attempt at the quantitative calibration of the signals. The measurements only provide a basis to compare the trends reported in this work with measurements reported elsewhere. They do however provide a convenient means to determine what frequency components are present in the plasma and how they vary with plasma parameters and plasma source settings.

2.2 Computational simulation

Computational simulations with a strongly coupled solution of Maxwell's equations and a fluid representation of the plasma[20] were used to obtain high-fidelity numerical predictions of the UHF electromagnetic wave content in the plasma for comparison with PAP measurements. Grid spacing and time increments satisfy the spatiotemporal resolution required to capture the UHF waves in the plasma and are shown to be well resolved up to the plasma frequency. The model used is also described elsewhere.[21,26] Briefly, the simulation employs a time domain solution of the magnetic vector potential representation of Maxwell's equations with the Coulomb gauge. The solution is fully coupled to the relevant equations for plasma kinetics with rates derived from an off-line solution of the zero-dimensional Boltzmann equation using the Bolsig+ software.[27] We

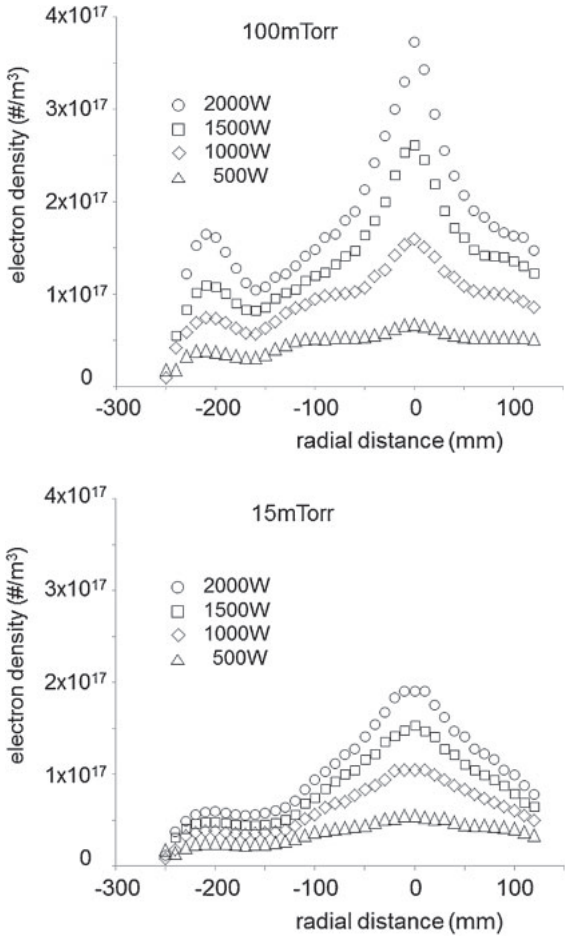

Fig. 3. Experimentally measured electron density profiles along the test-bench A reactor midgap for argon plasma driven at 60 MHz. Top: 100 mTorr. Bottom: 15 mTorr.

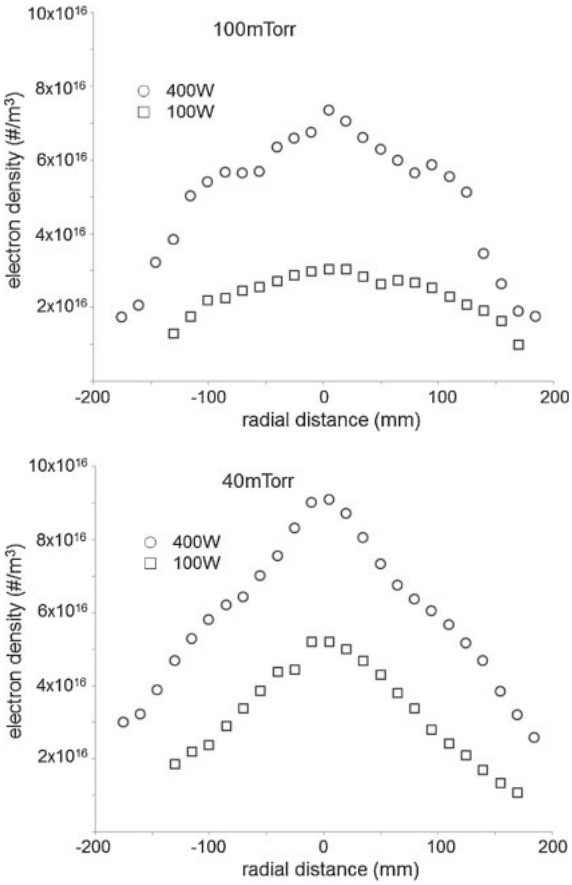

Fig. 4. Experimentally measured electron density profiles along the test-bench B reactor midgap for argon plasma driven at 106 MHz. Top: 100 mTorr. Bottom: 40 mTorr.

performed two-dimensional analysis because the higher harmonics exist only in the central regions, the diameter of which is several centimeters, and we did not find any mode of density profile in the θ-direction. The simulation enables us to resolve wave phenomena in the plasma up to the Nyquist limit, which is typically 10 GHz.

3. Experimental results

3.1 Electron density profile

In test-bench A, VHF power (60 MHz) was fed from the top electrode to pure Ar plasma. The bottom electrode and wall were grounded. Figure 3 shows the experimentally measured radial profiles of the electron number density along the midgap between the two parallel electrodes for 15 and 100 mTorr for this chamber. Center-peaked profiles can be observed over an applied VHF power range of 500–2000 W. For 100 mTorr and the lowest operating power (500 W), a broad and gentle center peak, the radial length scale of which is about 15 cm and the maximum electron number density is below 5×10^{16} ♯/m^3, is observed. However, when the VHF power is increased above 1000 W, an additional feature appears that is, a strong and relatively sharp center peak superimposed on the broad one. The sharp center peak becomes more prominent when the electron number density exceeds 1×10^{17} ♯/m^3, implying a narrow cylindrical region of intense plasma generation on axis. The radial length scale of the sharp center peak is a few centimeters. Although similar results can be observed at 15 mTorr, the center peak becomes broader owing to the increased diffusivity of the plasma species at the lower pressure. We know of no reports in the literature where the sharp center peak feature is reproduced by simulations for a 60 MHz driving frequency especially for electrodes with diameters as small as 200 mm.

The sharp-center-peaked electron density is not an artifact of a particular experimental system. In test-bench B, VHF power (106 MHz) was also fed from the top electrode to pure Ar gas plasma. The counter electrode and mesh exhaust were grounded. Once again, the primary difference is the proximity of the ground to the wafer susceptor edge. Figure 4 includes the measured electron density profile in the test-bench B reactor. For 100 mTorr and a lower power of 100 W where the electron number density is less than 4×10^{16} ♯/m^3, a broad peak, the radial length of which is about 15 cm, is observed. However, for 100 mTorr and a higher power of 400 W, the maximum electron number density exceeds 7×10^{16} ♯/m^3 and a sharp center peak is superimposed on the broad peak as observed in the test-bench A reactor. The radial length scale of the confined sharp center one is again a few centimeters. For a lower pressure of 40 mTorr and powers of 100–400 W, the sharp center peaks are also pronounced and their radial length scales are about 10 cm.

The experiments, taken together, show that increasing the RF power results in a sharp center electron density peak that

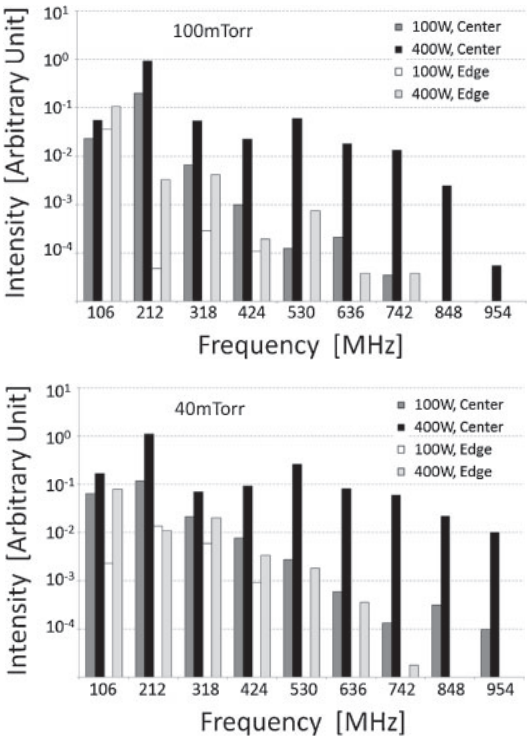

Fig. 5. Experimentally measured fast Fourier transform (FFT) of the axial electric fields in the midgap axial location of the test-bench B reactor for argon plasma driven at 106 MHz. Top: 100 mTorr. Bottom: 40 mTorr.

increases in magnitude relative to the broad peak electron density background. These conditions exist for a wide range of characteristic chamber dimensions: gap and ratio of substrate to grounded chamber wall diameters. A low pressure diminishes the sharpness of the density peak through diffusion.

3.2 Higher harmonic waves

The UHF content in the plasma bulk was measured in test-bench B (106 MHz) using a PAP for VHF powers of 100–400 W and pressures of 20–100 mTorr. Measurements were performed for different plasma conditions (frequency, power, and pressure) at the midgap height of the electrode center and electrode edge. As reported in our previous paper,[22] the skin depth ranges from 17.5 to 19 mm and the probe position is obviously at the skin depth where an evanescent electromagnetic wave can propagate. Because it is known from numerical simulation that the vertical component of an electromagnetic wave is stronger than the horizontal component, it is most likely that the vertical component of an evanescent electromagnetic wave is measured. In addition to the expected 2nd–4th harmonics of the fundamental,[12] 5th–9th (530–954 MHz) harmonics were observed and are presented in Fig. 5. These higher-order harmonics become prominent with increased power and correlate well with the magnitude of the sharp-center-peak of electron density.

For 100 mTorr and 100 W, the intensity of the 2nd harmonic is stronger than the fundamental at the center. The reverse is true at the plasma edge. The intensities of the 3rd (318 MHz)–7th (742 MHz) harmonics, which we call UHF waves, are negligible both at the center and edge with intensities far lower than the fundamental. The measured

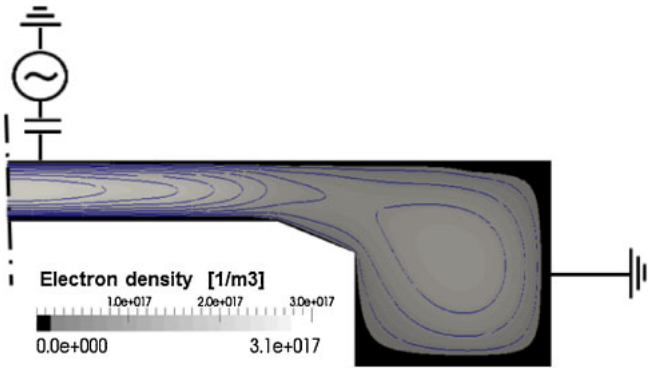

Fig. 6. (Color online) Computational results for the electron density in the test-bench A reactor for 100 mTorr argon plasma driven at 60 MHz.

profile of electron density in Fig. 4 shows a broad center peak and the radial length scale of this peak is about 15 cm. This broad center peak likely coincides with the presence of the fundamental and 2nd harmonics because the quarter wavelengths of those frequencies are 20 and 8 cm, respectively.[28] For 100 mTorr and 400 W, the tendency of the fundamental and 2nd harmonics is similar to the 100 W case. However, the 3rd (318 MHz)–7th (742 MHz) harmonics are prominent at the center but negligible at the edge. The experimentally measured electron densities presented in Fig. 4 show a sharp center peak at 100 mTorr and 400 W, the radial length scale of which is about 5 cm. The quarter wavelengths of the measured UHF waves are similar to the length scale ranging from 2 to 5 cm.

The intensities of UHF waves in the plasma for both 100 and 400 W at 40 mTorr are higher than those at 100 mTorr. In addition, the intensities of UHF waves at the center are higher than those at the edge under these conditions. Not surprisingly, the electron density profile becomes more sharply center-peaked. The UHF content and plasma density profile strongly correlate with each other.

4. Computational results

4.1 Electron density profile

The calculated electron density profile in the test-bench A reactor for 100 mTorr and 1000 W (60 MHz)[26] is presented in Fig. 6. The model results agree with the measured profile and enable us to replicate the confined sharp center peak and an off-center smaller peak near the chamber wall. Previous computational models reported in the literature that lack either the time-domain solution of Maxwell's equations or a sufficient mesh resolution (typically ~100 μm mesh resolution in the sheaths) have proven unable to demonstrate experimental results of the type discussed in this paper.

4.2 Higher harmonic waves

Figure 7 includes the calculated frequency spectrum of the electric field (vertical component) for the test-bench A reactor operating at 100 mTorr and 2000 W, which was obtained in plasma bulk where an evanescent electromagnetic wave can propagate. This spectrum is representative of those in experiments with a sharp center-peaked electron density. In addition, the fundamental, 2nd–4th harmonics, and UHF waves (>400 MHz) are prominent. Recall that Hebner et al.[2] reported that 4th and 5th (704–880 MHz) harmonics UHF

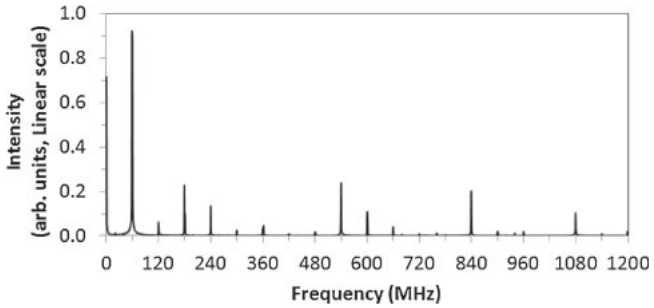

Fig. 7. FFT of computational simulation results for the axial electric fields in the midgap location of the test-bench A reactor for 100 mTorr argon plasma driven at 60 MHz.

waves exist only in the center region in the case of 176 MHz discharge and noted the correlation of the location of these UHF waves with a center-peaked plasma profile. Our simulation results are very likely a reproduction of the phenomena observed by Hebner et al.

Although we have shown the existence of higher harmonics electromagnetic waves, both experimentally and through computational modeling, the exact mechanism by which these wave are generated remains unclear. Some insights into the mechanism can however be gained through our computational model. We have often times found it necessary to add a small perturbation (artificial noise) to the input sinusoidal voltage waveform at the powered electrode in order to stabilize a plasma solution that predicts the center-peaked plasma profile (the previous simulation result discussed above required no artificial noise addition). This small perturbation of the numerical solution is similar to the perturbation required to trip turbulence in the direct numerical simulation of turbulent flows. A Gaussian white noise, comprising a spectrum of an infinite range of frequencies and with a few % voltage magnitude compared with the magnitude of the input fundamental excitation, is sufficient for the reliable prediction of the center-peaked profile in all simulations.

Here, we attempt to provide some insights into the generation of higher harmonics through the selective addition of higher harmonic perturbation signals superposed on the fundamental voltage excitation. For this part of the study, we performed simulations in a simple parallel-plate reactor geometry that is representative of the test-bench B reactor as shown in Fig. 8. The primary question posed was whether the small perturbation harmonic signals at various frequencies are amplified or damped by the plasma. A 2% voltage magnitude perturbation (compared with the fundamental excitation) was added to the 60 MHz fundamental in bands of three consecutive harmonics over the range from 2nd–19th harmonics. The frequency spectrum of the electric field in the plasma for one of the small perturbation additions in the 14th–16th harmonics is presented in Fig. 9. The high frequency perturbations are found to be amplified in the plasma as evident by the magnitudes of the fast Fourier transform (FFT) peaks at these harmonics. FFTs for the simulations with small perturbations added to all harmonics of 13th and lower show no amplification. The consequence of the amplification of the small perturbation addition can be seen in Fig. 10. Here, the electron density profiles with

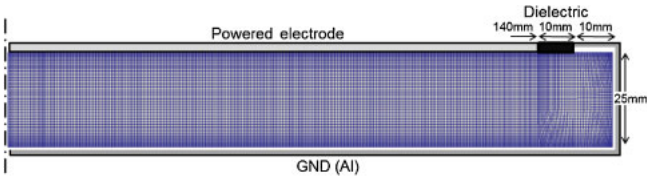

Fig. 8. (Color online) Schematic of a simple small cavity domain and the high-resolution computational mesh for the simulations.

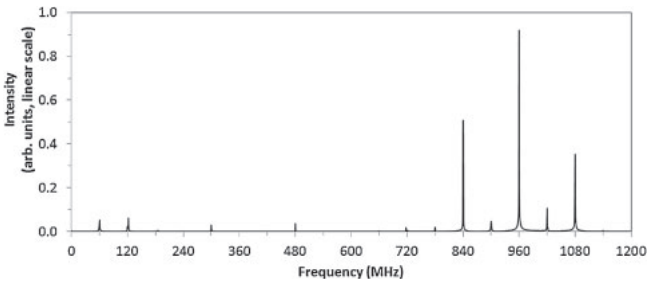

Fig. 9. FFT of the axial electric fields in the midgap axial location of the simple parallel plate reactor at 100 mTorr in the argon plasma. Here, a small perturbation with a 2% voltage magnitude is added in the 14th–16th harmonics of the fundamental excitation at 60 MHz.

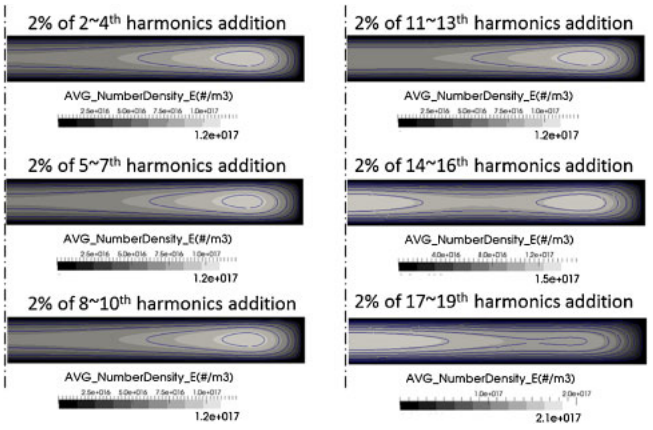

Fig. 10. (Color online) Computational results for the electron density in the cavity for 100 mTorr argon discharge driven at 60 MHz.

small perturbation additions in harmonic groups of 2nd–4th, 5th–7th, 8th–10th, 11th–13th, 14th–16th, and 17th–19th are shown. Consistent with the lack of amplification of perturbations for the 13th harmonic and lower, all cases with these perturbations show no center-peaked plasma profiles. However, all cases with voltage perturbations at the 14th harmonic and higher show a center-peaked plasma profile. Clearly, the presence of sources of small voltage perturbations at UHFs (14th harmonic and higher for 60 MHz fundamental excitation) and the amplification of these perturbations in the plasma are crucial to the understanding of the mechanism that generates center-peak density in VHF-CCP sources.

We do not show a parametric study of the impact of the chamber configuration, but note that the gap size and proximity of grounds to the driven electrode can induce other phenomena that may have strong impact in cases whether a center peak is observable or not. These phenomena may

include edge effects already well described in the literature and diffusion that we see in our own data playing a strong role. Overall, the computational results illustrate the importance of UHF waves produced in a VHF-CCP source. The UHF content above several hundred MHz coincides with the existence of a sharp-center-peaked electron density and may be amplified in the plasma itself.

5. Conclusions

Experimental measurements of the electron density profile and higher harmonic content of the electric field in VHF-CCP sources revealed that the confined sharp center peak superimposed on the broad center peak strongly correlates with the presence of UHF waves (400 MHz–1 GHz), although the frequencies of these waves are affected by the plasma density and chamber configuration. These results reproduce the experimental results obtained by Hebner et al.[2)] Complementing the experiments, precise numerical simulations of simple cavities and a full representation of our test-bench experiments indicate which harmonics are amplified in the plasma and produce the center peak. Power, pressure, frequency, and geometry determine the detailed profile, but it can be concluded that the center-peak evolution requires the amplification of the UHF wave content. The typical relationship between the UHF content in the plasma and the generation of the sharp center peak is clear from the simulation experiments where UHF waves were added. What remains to be clarified and is not described in this paper is how the UHF content evolves from the fundamental. This is the subject of an upcoming publication. At present, we exclude some effects. It is important to note that UHF waves at the frequencies of interest are not cut-off in the plasmas we are investigating. The skin depth is approximately half the gap dimension at the peak density, allowing axial propagation, and electromagnetic waves propagating radially may travel freely in the low-density plasma adjacent to the electrodes.

Acknowledgments

The authors express their gratitude to T. Ito and M. Vukovic who have provided advice and support during this work.

1) J. E. Stevens, M. J. Sowa, and J. L. Cecchi, J. Vac. Sci. Technol. A **14**, 139 (1996).
2) G. A. Hebner, GEC, RWI.00003 (2005).
3) P. A. Miller, E. V. Barnat, G. A. Hebner, A. M. Paterson, and J. P. Holland, Plasma Sources Sci. Technol. **15**, 889 (2006).
4) V. N. Volynets, A. G. Ushakov, D. Sung, Y. N. Tolmachev, V. G. Pashkovsky, J. B. Lee, T. Y. Kwon, and K. S. Jeong, J. Vac. Sci. Technol. A **26**, 406 (2008).
5) D. Sung, S. Jeong, Y. Park, V. N. Volynets, A. G. Ushakov, and G.-H. Kim, J. Vac. Sci. Technol. A **27**, 13 (2009).
6) H. Kokura, K. Nakamura, I. P. Ghanashev, and H. Sugai, Jpn. J. Appl. Phys. **38**, 5262 (1999).
7) K. Nakamura, M. Ohata, and H. Sugai, J. Vac. Sci. Technol. A **21**, 325 (2003).
8) T. Ito, Y. Mo, and H. Masahiro, GEC International Conf., Dallas (2008).
9) Y. Yamazawa, Appl. Phys. Lett. **95**, 191504 (2009).
10) M. A. Lieberman, J. P. Booth, P. Chabert, J. M. Rax, and M. M. Turner, Plasma Sources Sci. Technol. **11**, 283 (2002).
11) I. Lee, D. B. Graves, and M. A. Lieberman, Plasma Sources Sci. Technol. **17**, 015018 (2008).
12) M. A. Lieberman and A. J. Lichtenberg, *Principles of Plasma Discharges and Materials Processing* (Wiley, New York, 2005) 2nd ed., p. 411.
13) M. Klick, J. Appl. Phys. **79**, 3445 (1996).
14) T. Mussenbrock, D. Ziegler, and R. P. Brinkmann, Phys. Plasmas **13**, 083501 (2006).
15) D. Ziegler, T. Mussenbrock, and R. P. Brinkmann, Plasma Sources Sci. Technol. **17**, 045011 (2008).
16) D. Eremin, T. Hemke, R. P. Brinkmann, and T. Mussenbrock, J. Phys. D **46**, 084017 (2013).
17) U. Czarnetzki, T. Mussenbrock, and R. P. Brinkmann, Phys. Plasmas **13**, 123503 (2006).
18) T. Mussenbrock and R. P. Brinkmann, Appl. Phys. Lett. **88**, 151503 (2006).
19) T. Mussenbrock and R. P. Brinkmann, Plasma Sources Sci. Technol. **16**, 377 (2007).
20) VizGlow: Plasma Modeling Software for Multi-Dimensional Simulations of Non-Equilibrium Glow Discharge Systems, Theory Manual, version 1.9 (Esgee Technologies Inc., 2012).
21) I. Sawada, P. L. G. Ventzek, R. R. Upadhyay, B. Lane, T. Ohshita, and L. L. Raja, Dry Process Symp., 2013.
22) Y. Yang and M. J. Kushner, Plasma Sources Sci. Technol. **19**, 055011 (2010).
23) K. Bera, S. Rauf, K. Ramaswamy, and K. Collins, J. Vac. Sci. Technol. A **27**, 706 (2009).
24) S. Rauf, J. Kenney, and K. Collins, J. Appl. Phys. **105**, 103301 (2009).
25) M. J. Kushner, J. Phys. D **42**, 194013 (2009).
26) R. R. Upadhyay, I. Sawada, P. L. G. Ventzek, and L. L. Raja, J. Phys. D **46**, 472001 (2013).
27) G. J. M. Hagelaar and L. C. Pitchford, Plasma Sources Sci. Technol. **14**, 722 (2005).
28) P. Chabert, J.-L. Raimbault, P. Levif, J.-M. Rax, and M. A. Lieberman, Plasma Sources Sci. Technol. **15**, S130 (2006).